

## Top Background to SM Higgs Searches in the $W^+W^- \rightarrow \ell\nu\ell\bar{\nu}$ Decay Mode at CMS

---

**G.Davatz**

*Institute for Particle Physics, ETH Zurich, Switzerland*

**A.S. Giolo-Nicollerat**

*CERN, Geneva, Switzerland*

**M.Zanetti\***

*Dipartimento di Fisica “Galileo Galilei” and INFN, Padova, Italy*

The top quark and its properties within and beyond the Standard Model will be extensively studied at the incoming Large Hadron Collider. Nonetheless the top quark will play the role of the main background for most of the Higgs and new physics searches. In this paper the top as a background to  $H \rightarrow W^+W^- \rightarrow l^+\nu l^-\bar{\nu}$  Higgs discovery channel will be studied. The current status of the Monte Carlo tools for  $t\bar{t}$  and single top simulation will be presented. Finally the problem on how to evaluate the top background from the data will be addressed and the related systematics will be discussed.

*Top2006, Coimbra, Portugal*

---

\*Speaker.

## 1. Introduction

At the Large Hadron Collider (LHC), the production cross section for processes involving the top quark, either in the singly and the doubly resonant mode, is foreseen to exceed 1 nb (respectively  $\sim 0.3$  nb for single top and  $\sim 0.8$  nb for  $t\bar{t}$ ). At the designed instantaneous luminosity of  $\mathcal{L} = 10^{34} \text{ cm}^{-2}\text{s}^{-1}$ , averagely more than 10 events containing top per second are expected. In this sense the LHC will be a top factory allowing to study with no statistical limitation the properties of the most peculiar particle discovered so far. Moreover, providing copiously most of the detectors' observables like (b-)jets, leptons, missing transverse energy ( $E_T^{\text{miss}}$ ) etc. , top events will be a candle for the comprehension of various experimental systematics and detector performances. Nevertheless, at the same time, the top quark will play the role of background for most of the Higgs and new physics signatures.

Studying the top quark as a background instead as a signal is clearly a complete different issue that needs different experimental and theoretical approaches with consequent specific systematics uncertainties. Moreover, the phase space where the top plays the role of the background is usually narrow and contains only the tails of the events' distributions.

In this paper the top background to the  $H \rightarrow W^+W^- \rightarrow l^+\nu l^-\bar{\nu}$  Higgs discovery channel will be studied in details for the case of the CMS detector.

In the first section, a brief overview of the characteristics of the signal and the top background will be given. The following part will focus on the simulation of the top events; the generation of  $t\bar{t}$  events will be studied by comparing different Monte Carlo programs, then the inclusion of singly resonant top production at Next to Leading Order (NLO) will be discussed.

The LHC energy regime has never been probed so far, thus any sound analysis must rely on measured data to the maximum extent. In the second part, the problem on how to normalize the top background using data will be addressed. Finally the experimental uncertainties coming from different normalization strategies will be estimated using a full CMS simulation.

## 2. The $H \rightarrow WW \rightarrow \ell\nu\ell\nu$ and the top background

At the LHC, the  $H \rightarrow W^+W^- \rightarrow l^+\nu l^-\bar{\nu}$  Higgs decay mode is considered the most favorable one for a Higgs mass ranging between 150 – 170 GeV [1] [2]. This can be argued from the right plot in Figure 1, showing the statistical significance foreseen with  $30 \text{ fb}^{-1}$  at CMS for the various Higgs channels as a function of  $m_H$ .

The signal is characterized by two isolated, high  $p_T$  and nearby leptons with small invariant mass, an high value of  $E_T^{\text{miss}}$  and no reconstructed jet in the central part of the detector. The main backgrounds are the non-resonant  $W$ -pair, the Drell Yan, the  $t\bar{t}$  and the single top in the  $Wt$  mode<sup>1</sup>.

The variable that allows to discriminate the irreducible background from continuous  $W$ -pair production is the opening angle between the leptons. Due to scalar nature of the Higgs, the  $W$  bosons are produced mainly with opposite helicity, then, because of the V-A structure of the  $W$ s coupling to leptons, the latters are produced nearby in the space. In the left plot of Figure 1 the opening angle between the leptons are shown for the signal and the  $q\bar{q} \rightarrow W^+W^-$  process. Since the angular

<sup>1</sup>One may think to consider the complete gauge invariant process  $W^+bW^-\bar{b} \rightarrow l^+\nu bl^-\bar{\nu}\bar{b}$  instead of keeping separate  $t\bar{t}$  and  $tWb$ . The reason why this is not done will be given in section 4

distributions of the leptons are crucial variables, the top polarization should be taken into account throughout its whole decay chain by the Monte Carlo generators. This issue will be addressed in 3.3

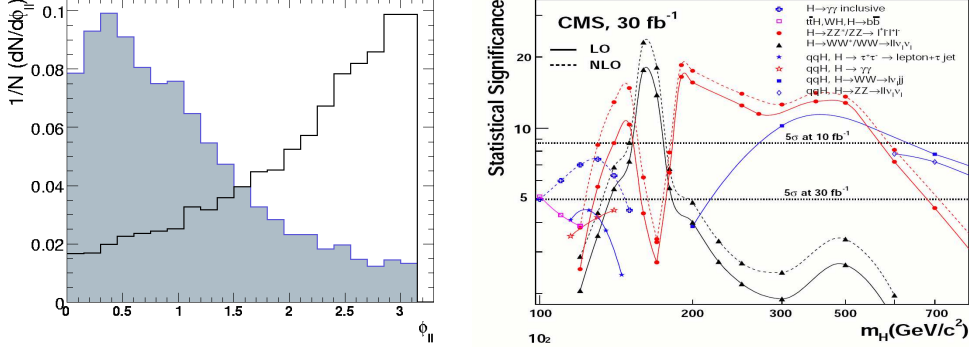


**Figure 1:** Left: opening angle between the leptons ( $\phi_{\ell\ell}$ ) for the signal (blue) and the  $W$ -pairs background (black). Right: statistical significance foreseen with  $30 \text{ fb}^{-1}$  at CMS for various Higgs channels as a function of  $m_H$ .

The most powerful cut to reduce the top events is the jet veto which requires not to have reconstructed jets above a certain  $E_T$  threshold in the central part of the detector. Dealing with low  $E_T$  jets in the LHC environment is a delicate issue either from the experimental and from the theoretical point of view. More details about this selection will be given in 5.1. When the problem of the NLO description of  $Wt$  will be addressed, it will also be remarked how the application of a jet veto helps in consistently separate this process from  $t\bar{t}$ .

		$H \rightarrow WW$ ( $m_H = 165 \text{ GeV}$ )	$t\bar{t}$	$tWb$
	$\sigma \times \text{BR}(e, \mu, \tau)$ [fb]	2360	86200	3400
1)	Trigger	1390 (59%)	57380 (67%)	2320 (68%)
2)	lepton ID	393 (28%)	15700 (27%)	676 (29%)
3)	$E_t^{\text{miss}} > 50 \text{ GeV}$	274 (70%)	9332 (59%)	391 (58%)
4)	$\phi_{\ell\ell} < 45$	158 (58%)	1649 (18%)	65 (17%)
5)	$12 \text{ GeV} < m_{\ell\ell} < 40 \text{ GeV}$	119 (75%)	661 (40%)	28 (43%)
6)	$30 \text{ GeV} < p_t^{\ell \text{max}} < 55 \text{ GeV}$	88 (74%)	304 (46%)	13 (46%)
7)	$p_t^{\ell \text{min}} > 25 \text{ GeV}$	75 (85%)	220 (73%)	9.2 (71%)
8)	Jet veto	46 (61%)	9.8 (4.5%)	1.4 (15%)

**Table 1:** The expected number of events for a luminosity of  $1 \text{ fb}^{-1}$  for the signal with a Higgs mass of 165 GeV and the  $t\bar{t}$  and  $tWb$  background. The relative efficiency with respect to the previous cut is given inside the brackets in percent.

In Table 1 the complete list of selections used together with the corresponding number of events expected for  $1 \text{ fb}^{-1}$  for the fully simulated signal (for a Higgs mass of 165 GeV),  $t\bar{t}$  and  $Wt$  are summarized. The rejection for  $t\bar{t}$  is  $\mathcal{O}(10^{-4})$ , which sets a challenge for the needed precision of the Monte Carlo calculations. Moreover the presence of two neutrinos in the signal final state

does not allow the reconstruction of a narrow invariant mass peak; the discovery has then to rely on an excess in the expected number of background events. It is thus necessary to identify a phase space region where reliably control the contribution of the different backgrounds. In section 5, two procedure for the  $t\bar{t}$  normalization are proposed and discussed.

### 3. $t\bar{t}$ background generation

In this section the generation of top-pair process ( $pp \rightarrow t\bar{t} \rightarrow WbW\bar{b} \rightarrow \ell\nu\ell\nu b\bar{b}$ , with  $\ell = e, \mu$  and  $\tau$ ) will be discussed by comparing four different Monte Carlo (MC) generators. Three points will be addressed: first we will estimate how much the Born level description differs from the NLO one in the phase space relevant for the Higgs search. Then we will determine whether different showering models cause differences in the relevant kinematics distributions. Finally how much the inclusion of the spin correlation between the top quarks affects the leptons' angular distribution will be estimated. All the following studies have been done at parton level, without exploiting a full detector simulation.

#### 3.1 NLO effects on $t\bar{t}$ simulation

To estimate the effect of an accurate inclusion of NLO matrix elements, HERWIG 6.508 [3] (LO, parton shower Monte Carlo) and MC@NLO 2.31 [4] (NLO, parton shower Monte Carlo) were compared. The spin correlations between the  $t$  and  $\bar{t}$  are not considered in MC@NLO. HERWIG events were therefore consistently simulated without such correlation. As the same showering model is used, the difference between the two simulations should be mostly due to the additional NLO matrix elements in MC@NLO.

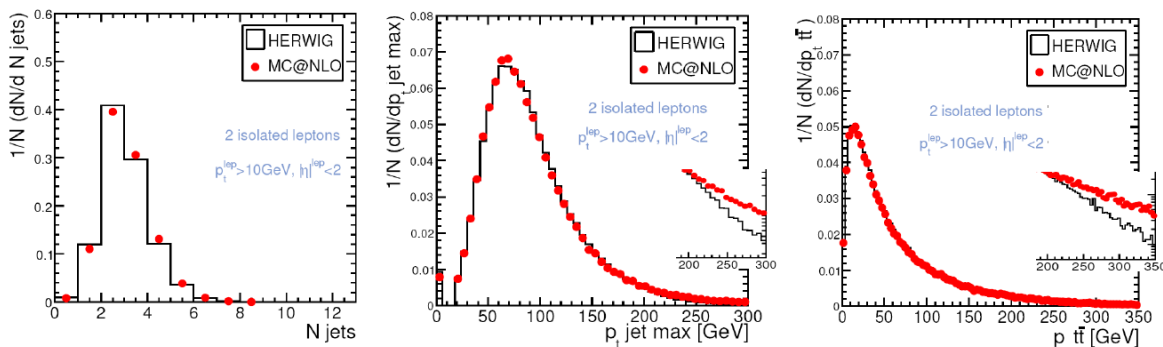


**Figure 2:** Left: jet multiplicity. Center: leading jet  $E_T$ . Right: transvers momentum of the  $t\bar{t}$  system. The little windows in the center and right plots show the deviation at high  $p_T$  in logarithmic scale.

In Figure 2, from left to right, the number of jets, the  $E_T$  of the leading jet and the  $p_T$  of the  $t\bar{t}$  system are shown<sup>2</sup>. MC@NLO produces in addition to the hard process up to one hard jet whose spectrum is accurate at NLO. Most of the jet activity in the events is however dominated by the two b-quarks from the two top quarks decay. None of the three distributions shows indeed relevant differences between the NLO and LO. Typical NLO effects can be noticed in the high part of the

<sup>2</sup>this variable gives an estimation of the spectrum of the additional jets to the hard process

spectrum either in the leading jet  $E_T$  distribution and in the  $t\bar{t}$  system transverse momentum: the parton shower is in fact known to describe correctly only the soft part of the extra jet activity. Nevertheless the region relevant for the  $H \rightarrow WW \rightarrow \ell\nu\ell\nu$  signal selection is the very low  $p_T$  region, where HERWIG and MC@NLO agree very well. In addition, the shapes of all the other cut variables are very similar in MC@NLO and HERWIG without spin correlations.

When comparing the relative efficiencies of the different cuts, the two Monte Carlos differ essentially only for the jet veto cut, the difference in the efficiency being  $\mathcal{O}(10\%)$  [5]. Since the region where NLO makes a difference is at very high  $p_T$ , whereas the bulk of the selected events is in the low  $p_T$  region, it is safe to conclude that NLO effect can be simply included by rescaling the cross section by an inclusive factor.

### 3.2 Effect of showering models, differences between HERWIG and PYTHIA

In the following, how different showering models influences the variable shapes and selection efficiencies will be studied. For this, PYTHIA 6.325 [6], based on the Lund hadronization model, was compared with HERWIG based on the cluster model for hadronization<sup>3</sup>. For both simulations, default scales were chosen.

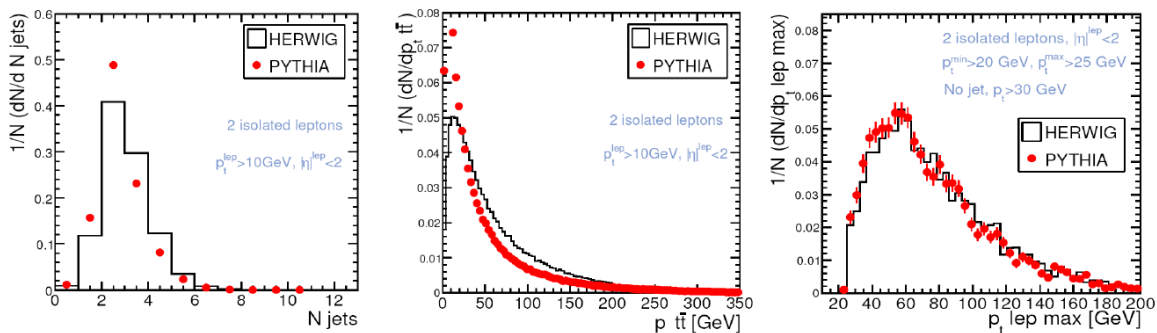


**Figure 3:** Left: jet multiplicity. Center:  $t\bar{t}$  system  $p_T$ . Right:  $p_T$  of the most energetic lepton after the jet veto

The left and central plots of Figure 3 shows respectively the number of jets and the  $p_T$  of the  $t\bar{t}$  system. The two showering models differ remarkably in both distributions, the Lund model predicting less and softer extra jets. The effect of these discrepancies in the jet veto efficiencies is sizable, i.e. about 20%.

However, the shapes of the relevant leptons' kinematics distributions in the signal region are very similar for the two Monte Carlo's. This can be seen from the right plot of of Figure 3 showing the  $p_T$  spectrum of the most energetic lepton after applying the jet veto.

### 3.3 Effect of the spin correlations

As explained in 2, the variable that characterizes more the signal is the opening angle between the two leptons. This observable, as well as the mass of the dilepton system and the  $E_T^{\text{miss}}$ , is

<sup>3</sup>PYTHIA does not take into account the spin correlations between the top and the anti-top, then in order to consistently study only the differences caused by the showering model, HERWIG with disabled spin correlations has been used

sensitive to the spin correlations between the particles involved in the process. In order to point out the effect of the inclusion of the top polarization in the  $t\bar{t}$  decay chain on the leptons' angular distribution, PYTHIA has been compared with TopREX [7]. While the former does not consider the top spin along its decay, the latter is a matrix element based Monte Carlo describing exactly  $2 \rightarrow 6$  processes with LO precision.

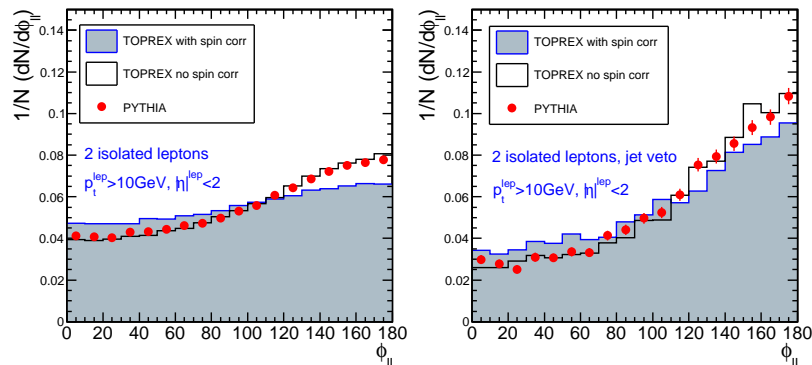


**Figure 4:**  $\phi_{\ell\ell}$  distribution for TopREX events with and without spin correlations is shown, as well as PYTHIA. On the left, only very basic cuts are applied, whereas on the right a jet veto is applied in addition. The region important for the Higgs signal search is the low  $\phi_{\ell\ell}$  region.

In the left plot of Figure 4 showing the angle  $\phi_{\ell\ell}$  between the leptons a non negligible difference between the two Monte Carlo's prediction can be seen. Quantitatively, the variation of the efficiency for the  $\phi_{\ell\ell}$  cut between the PYTHIA and TopREX is  $\sim 10\%$ . As it can be seen from the right plot of Figure 4, in the signal region, i.e. after applying the jet veto, the difference between the two distributions, even if still present, tends to flat.

#### 4. Singly resonant top background generation

Although the  $Wt$  mode of the single top production has an estimated cross section one order of magnitude times smaller than the  $t\bar{t}$  production, the application of the jet veto enhances the contribution of the former with respect to the latter's. Considering also that the single top process has never been measured at the Tevatron, it is important to pursue a NLO description of this process that allows a precise estimation of its features and its total cross section. In principle one could think to use the singly and doubly resonant processes together i.e. to consider  $pp \rightarrow WbWb \rightarrow \ell\nu\ell\nu b\bar{b}$  which is naturally gauge invariant and describes correctly all the interference terms. Nevertheless the NLO corrections are not available for such a process and in particular it is not known how to deal with the arising large logarithms of the form  $\log((m_t + m_W)/m_b)$ . It is therefore preferable to view the singly resonant process as one in which a b quark is probed directly inside the proton [8] (right diagram in Figure 5).

The diagrams contributing to the NLO description of  $Wt$  includes the LO doubly resonant  $t\bar{t}$  (left diagram in Figure 5). A solution to that has been provided by Campbell and Tramontano in Ref. [9] where they suggest to define a specific  $Wt$  final state by imposing a veto on the presence of an extra b quark. In this schema, also called "b-PDF approach", the  $p_T$  threshold for the spectator

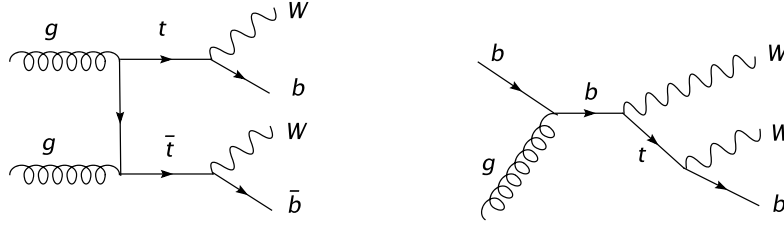


**Figure 5:** Examples of Feynman graphs for double (left) and single (right) top production

b-quark (coming from an initial gluon splitting) is set at the same value of the factorization scale used for the PDF.

This approach perfectly fits with the case of the  $Wt$  background for the  $H \rightarrow W^+W^- \rightarrow l^+ \nu l^- \bar{\nu}$  searches where a global jet veto is applied. In Ref. [5] the efficiencies for  $Wt$  events for the signal leptons' selections have been compared between LO plus parton shower (TopREX + PYTHIA) and NLO (MCFM [10]) descriptions, showing an overall agreement. After matching the veto threshold on the b-quark with the threshold for the jet veto, it is possible to consistently use the overall normalization provided by the NLO calculation for the cross section in the signal phase space area. The ratio between the LO and NLO cross section goes from 1.4 before the application of the cuts, to 0.7 after the selection. This is consistent with the fact that NLO calculations enhances the jet activity thus reducing the jet veto efficiency.

## 5. $t\bar{t}$ normalization from data

The commonly used method to normalize a given background from the data consists on selecting a signal-free phase space region (control region) where a given background process is enhanced. The contribution of that background in the signal region is then extrapolated from the measured amount of events in the control region. This procedure relies on the relation:

$$N_{signal\_reg} = \frac{N_{signal\_reg}^{MonteCarlo}}{N_{control\_reg}^{MonteCarlo}} N_{control\_reg} = \frac{\sigma_{signal\_reg} \cdot \epsilon_{signal\_reg}}{\sigma_{control\_reg} \cdot \epsilon_{control\_reg}} N_{control\_reg} \quad (5.1)$$

where  $N_{signal\_reg}^{MonteCarlo}$  and  $N_{control\_reg}^{MonteCarlo}$  are the numbers of events predicted by the Monte Carlo simulation in the signal and control region. Each of this two numbers can be expressed as a product of the theoretical cross section in that phase space area,  $\sigma_{signal\_reg,control\_reg}$ , and the experimental efficiency of reconstructing events in the same region,  $\epsilon_{signal\_reg,control\_reg}$ <sup>4</sup>. This will allow to better point out the different sources of systematic uncertainties. In particular the theoretical predictions enter the procedure only via the ratio  $\sigma_{signal\_reg}/\sigma_{control\_reg}$ , leading to a much smaller scale dependency and thus to smaller theoretical uncertainties.

The theoretical issues concerning the  $t\bar{t}$  normalization have been deeply studied in [13], following the work done in the 2003 Les Houches Workshop. The primary goal here is to provide a reliable

<sup>4</sup>The experimental uncertainties could modify the boundaries defining the phase space where the cross section is calculated theoretically. This is the case in particular when the selections involve jets. The “ $\epsilon$ ” terms in relation (5.1) are assumed to account also for this effect.

description of the experimental aspects, specifically the ones related to the CMS detector. For this study a full detector simulation has then been exploited.

The main requirement from the experimental side on the choice of the control region is to limit as much as possible the error due to the “ $\epsilon$ ” terms in relation (5.1). This implies to use similar selections as for the signal region. Moreover the contamination from other physical and instrumental backgrounds should be negligible.

In the following the signal phase space area and two possible control regions for  $t\bar{t}$  normalization are described, focusing on the related experimental issues. Each of these phase space regions (either the signal and the control ones) is defined by the selections on the leptons listed in Table 1 (items 1-8).

### 5.1 Signal region

We already stated before that the signal region is defined by requiring not to have reconstructed jet above a certain  $E_T$  threshold in the central part of the detector. Clearly the lower the  $E_T$  threshold, the higher is the rejection for  $t\bar{t}$  background events. At CMS the definition of a jet at low  $E_T$  is experimentally problematic. This because the 4 Tesla magnetic field of the CMS solenoid spread the jet constituents in the transverse plane and prevents the low momentum charged tracks produced during the fragmentation even to reach the calorimeters. Moreover the LHC, in addition to the products of the hard scattering, produces thousands of charged and neutral particles some of which may have rather high  $p_T$ , thus enhancing the jets fake rate.

In order to avoid a high rate of fake jets at low  $E_T$ , the tracking measurements are exploited in the jet definition. For jets between 15 and 20 GeV the sum of the  $p_T$  of the tracks belonging to the jets (i.e. the tracks coming from the primary vertex which stand within the jet cone) is required to be at least the 20% of the jet  $E_T$  [2].

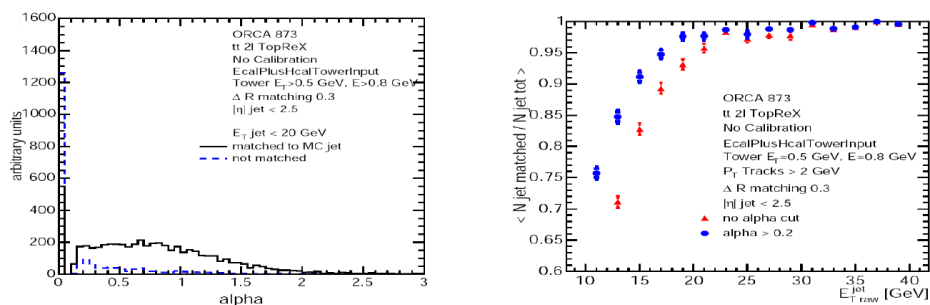


**Figure 6:** Left:  $\alpha$  distribution for matched and un-matched jets. Right: fraction of matched jets as a function of the reconstructed jet  $E_T$

As it can be seen from the right plot in Figure 6, the fake jets (i.e. not matched with any jet at parton level) rate below 20 GeV decreases remarkably. The distribution of  $\alpha = \sum p_T(\text{tracks})/E_T(\text{jet})$  from matched and un-matched jets is shown in the left plot of Figure 6.

### 5.2 b-tagging jets based $t\bar{t}$ control region

The request for two b-tagged jets is the most natural for the definition of a control region for the  $t\bar{t}$  background. In this study, the algorithm used to discriminate whether a jet is originated from



a  $b$  quark is based on the impact parameters of charged particle tracks associated to the jet [11]. The parameter that characterizes the efficiency and the mistagging rate of the algorithm is the impact parameter significance ( $\sigma_{IP}$ ) of a minimum number of tracks associated to the jet. In this study a jet is tagged as a  $b$ -jet if its measured  $E_t$  is greater than  $20 \text{ GeV}$  and if there are at least 2 tracks whose  $\sigma_{IP}$  is greater than 2. In this case the double  $b$ -tagging efficiency is  $\mathcal{O}(30\%)$  while the mistagging rate is  $\mathcal{O}(3\%)$ . Table 2 summarizes the number of events expected for  $10 \text{ fb}^{-1}$  in the control region for  $t\bar{t}$ ,  $Wt$  and the signal in the case of  $2\mu$ ,  $2e$  and  $e\mu$  final states.

Not all the processes with  $2\ell + 2b + E_t^{miss}$  as final state have been fully simulated for this analysis, nevertheless general considerations and fast Monte Carlo level checks can lead to exclude other relevant sources of backgrounds.

The more natural concurrent process is the not resonant  $W^+W^- \rightarrow 2\ell + b\bar{b}$  which is anyway suppressed with respect to  $t\bar{t}$ . Its cross section is indeed expected to be smaller than  $1 \text{ pb}$ . Assuming the same efficiency for the kinematic selections as for the  $W^+W^- \rightarrow 2\ell$ , i.e.  $\mathcal{O}(10^{-3})$ , less than 10 events are expected for  $10 \text{ fb}^{-1}$  in the control region even without folding the double- $b$  tagging efficiency. In the case of same flavor leptons in the final state,  $\gamma^*/Z^* \rightarrow 2\ell + b\bar{b}$  (the vector boson mass being away from the  $Z$  peak, i.e.  $m_{\ell\ell} < 40 \text{ GeV}$ ) could also contribute as an instrumental background, when an high value of  $E_t^{miss}$  is provided by the not full hermeticity of the detector and/or due the finite resolution of the calorimeters. Anyway for a fully simulated sample of  $\gamma^*/Z^* \rightarrow 2\ell + 2b$  with jets'  $E_t$  greater than  $20 \text{ GeV}$ , the fraction of events with  $E_t^{miss} > 50 \text{ GeV}$  (the actual cut applied for the signal selection) is  $\mathcal{O}(10^{-2})$ . Applying the same kinematic selections, but the  $E_t^{miss}$  cut on a  $pp \rightarrow \gamma^*/Z^* \rightarrow 2\ell + b\bar{b}$  sample generated with MadGraph Monte Carlo [12], 200 events are expected for  $10 \text{ fb}^{-1}$ , which reduce to a negligible quantity if the rejection due to a realistic  $E_t^{miss}$  selection is included<sup>5</sup>.

### 5.3 Two high $E_t$ jets based $t\bar{t}$ control region

In order to avoid the systematics due to the  $b$ -tagging algorithm it is worth to have alternative methods to estimate the  $t\bar{t}$  background from data. Each of the two  $b$ 's in the  $t\bar{t}$  final state come from a  $175 \text{ GeV}$  central object; their  $E_t$  spectra are then rather hard. An alternative method to define a  $t\bar{t}$  control region is thus simply to require, in addition to the signal kinematic cuts listed in Table 1, two hard jets in the detector.

In order to avoid the contamination from Drell Yan which in the case of  $2\ell + 2j$  final state has a much higher cross section than the  $2\ell + 2b$  one, only  $e\mu$  final state has been considered.

The thresholds on the jets' transverse energy that maximize the signal ( $t\bar{t}$ ) over the background ( $Wt$ +signal) ratio and minimize the statistical error have been found to be  $50$  and  $30 \text{ GeV}$ . The number of events expected events for  $10 \text{ fb}^{-1}$  for  $t\bar{t}$ ,  $Wt$  and the signal are summarized in Table 2.

A background process not considered in the full simulation analysis is  $W^+W^- \rightarrow \mu \nu_\mu + e \nu_e + 2j$ . The cross section, after geometrical acceptance cuts, is  $0.4 \text{ pb}$ , whereas the signal selection cuts efficiency resulted to be smaller than  $5 \cdot 10^{-4}$  (with a statistical error of  $\sim 8\%$ ). The contribution of this background can then be assumed to be at maximum of the order as the signal.

---

<sup>5</sup>In the  $\gamma^*/Z^* \rightarrow 2\ell + 2b$  fully simulated sample (the only one available) the  $b\bar{b}$  pair comes only from a gluon splitting, the main mechanism of  $\gamma^*/Z^* + 2b$  not being included. That is the reason why the selection cuts have been applied at parton level on a MadGraph sample

	“b-tagging” control region			“hard jets” control region			Signal region		
	$2\mu$	$2e$	$e\mu$	$2\mu$	$2e$	$e\mu$	$2\mu$	$2e$	$e\mu$
$t\bar{t}$	194	107	245	-	-	411	33	22	44
$Wt$	1	< 1	2	-	-	6	5	3	6
Signal ( $m_H = 165$ )	< 1	< 1	1	-	-	11	156	89	214

**Table 2:** Number of events of  $t\bar{t}$ , Signal and  $Wt$  expected for  $10 \text{ fb}^{-1}$  in the two control regions described above and in the signal region. Results are shown for  $2\mu$ ,  $2e$ ,  $e\mu$  final states.

In the case one jet is misidentified as an electron,  $W^\pm \rightarrow \mu \nu_\mu + 3j$ , could be a source of background too. At CMS, the probability of electron misidentification is estimated to be  $\mathcal{O}(10^{-4})^6$ . Given its cross section, calculated to be  $\sim 200 \text{ pb}$  after the geometrical acceptance cuts, the latter rejection factor together with the kinematic selection efficiency -estimated again from a generator level study to be  $\mathcal{O}(10^{-4})$ - lead to neglect this process as a source of contamination of the  $t\bar{t}$  control region.

## 6. $t\bar{t}$ normalization procedure uncertainties

Our proposed procedures to estimate the number of  $t\bar{t}$  events in the signal phase space region exploits relation (5.1). In order to compute the systematic uncertainties on the final result we consider separately those related to each term present in the formula.

### Theoretical uncertainty.

Taking the ratio of the  $t\bar{t}$  cross sections in the signal and control region avoids much of the theoretical systematic uncertainties. In Ref. [13] the theoretical uncertainty on the ratio  $\sigma_{\text{signal\_reg}}/\sigma_{\text{control\_reg}}$  has been studied at parton level with LO precision by varying the renormalization and factorization scale. The error has been estimated to range between 3% to 10%, mostly due to the choice of the PDF. For what it has been shown before, the theoretical error can be larger because of other factors, mainly the parton shower model. A 10% systematical error due to theoretical uncertainty will be assumed as reported in Ref. [13], although baring in mind that this could be an optimistic estimation.

### Jet Energy Scale uncertainty.

In the background normalization procedures we proposed, the jet energy scale (JES) uncertainty is particularly important since it affects in opposite manners the signal region, defined by vetoing the jets, and the control region where the presence of two jets is required. To take into account this sort of anticorrelation of  $\varepsilon_{\text{signal\_reg}}$  and  $\varepsilon_{\text{control\_reg}}$ , we estimate the effect of the JES uncertainty directly on their ratio by rescaling the measured jet four momentum by an amount corresponding to the percentual uncertainty (i.e.  $P_{\text{jet}}^\mu = (1 + \lambda)P_{\text{jet}}^\mu$ ).

In the plot of Figure (7) the relative variation of  $\frac{\varepsilon_{\text{signal\_reg}}}{\varepsilon_{\text{control\_reg}}}$  for various values of  $\lambda$  is shown. In the plot the triangles represent the control region defined by requiring two jets with  $E_t$  greater then 50

<sup>6</sup>The muon misidentification rate is at least one order of magnitude smaller

and 35 GeV, whereas the squares stand for the control region defined by requiring two b-tagged jets<sup>7</sup>. A realistic estimation of the JES uncertainty at CMS after integrating  $10 fb^{-1}$  of LHC is  $\mathcal{O}(5\%)$ . The the corresponding relative variation of  $\epsilon_{\text{signal\_reg}}/\epsilon_{\text{control\_reg}}$  is  $\sim 8\%$  for the double b-tagging defined control region and  $\sim 10\%$  for the two high  $E_t$  jets control region.

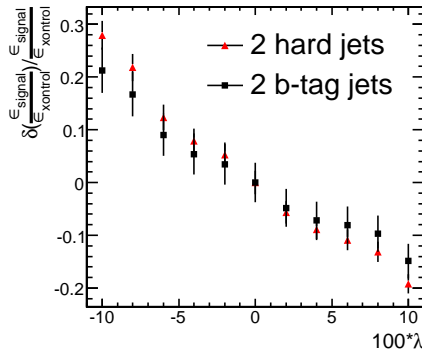


**Figure 7:** Relative variation of  $\frac{\epsilon_{\text{signal\_reg}}}{\epsilon_{\text{control\_reg}}}$  as a function the jet momentum rescaling factor ( $\lambda$ ). The red triangles represent the control region defined by two hard jets whereas the black squares correspond to the two b-tagged jets phase space area.

#### $\alpha$ criterion uncertainty.

To estimate the systematic uncertainty due to  $\alpha$  criterion, the value of the cut has been varied from 0.15 to 0.25. Moreover different values of the minimum  $p_t$  for a track to be included in the sum have been tried, from 2 to 3 GeV. The consequent variation of the jet veto efficiency ( $\epsilon_{\text{signal\_reg}}$ ) is relatively small, i.e. of the order of 4%.

#### b-Tagging uncertainty.

In Ref. [14] the precision with which the b-tagging efficiency will be known at CMS is expected to be 11% for  $1 fb^{-1}$  integrated luminosity and it is foreseen to improve till 7% with  $10 fb^{-1}$ . These values represent directly the uncertainty on  $\epsilon_{\text{control\_reg}}$  in the case of the control region defined by requiring two b-tagged jets.

#### Uncertainties on $N_{\text{control\_reg}}$ .

It has been shown in the previous section that  $t\bar{t}$  is plainly the dominant process in both the proposed control regions. In the worst case, i.e. when the control region is defined by two high  $E_t$  jets, the fraction of events coming form other processes is smaller than 4%. Provided that this fraction is small, it is safe to simply neglect this source of systematic.

For  $10 fb^{-1}$  the experimental uncertainties listed above accounts for a systematic error of  $\sim 11\%$  for both the  $t\bar{t}$  control regions. Including the theoretical uncertainty this error does not exceed 16%.

<sup>7</sup>The reason way the ratio  $\epsilon_{\text{signal\_reg}}/\epsilon_{\text{control\_reg}}$  in the latter case is less sensitive to the JES uncertainty is that the  $E_t$  threshold for the b-jets candidates is 20 GeV and the fraction of  $t\bar{t}$  events with b-tagged jets with  $E_t$  close to that threshold is very small.

## Statistical uncertainties

The statistical precision with which the number of  $t\bar{t}$  events in the signal region can be known depends on the expected number of  $t\bar{t}$  events in the control region. From the numbers quoted in Table 2, assuming a poissonian behavior, it is clear that the error due to systematic uncertainties is predominant with respect to the statistical ones for both the proposed normalization procedures.

## 7. Conclusions

The searches for the Higgs boson at the LHC via the channel  $H \rightarrow W^+W^- \rightarrow l^+ \nu l^- \bar{\nu}$  offers the possibility to study the  $t\bar{t}$  and  $Wt$  in a peculiar phase space region. This represents a major challenge either from the theoretical and from the experimental point of view.

The present status of the Monte Carlo tools for  $t\bar{t}$  simulation has been discussed. The comparison between a set of generators shows that the NLO effects can be safely accounted as a global rescaling of the total cross section. On the contrary the PYTHIA and HERWIG showering models differ in predicting jets multiplicity and energy spectra. Finally the spin correlation between the top-pair induces a variation of  $\mathcal{O}(10\%)$  in the leptons' selection cuts efficiency. In section 4 it has been show that the  $Wt$  process can be reliably calculated at NLO in the signal region defined by a jet veto without double counting with  $t\bar{t}$ .

Finally the normalization of the  $t\bar{t}$  background have been discussed. Two control regions have been proposed, one based on b-tagging the jets coming from the top-pair and the other by requiring two high  $E_T$  jets. Both approaches provide a reliable phase space area dominated by  $t\bar{t}$  events and lead to an overall systematic uncertainty of 16%.

## References

- [1] M. Dittmar and H. K. Dreiner, *How to find a Higgs boson with a mass between 155-GeV to 180-GeV at the LHC*, Phys. Rev. D **55** (1997) 167 [arXiv:hep-ph/9608317].
- [2] G. Davatz, M. Dittmar, A.S. Giolo Nicollerat, *Standard Model Higgs Discovery Potential of CMS in the  $H \rightarrow WW \rightarrow \ell\nu\ell\nu$  Channel*, **CMS NOTE-2006-048**.
- [3] G. Corcella *et al.*, *HERWIG 6.5 release note*, [arXiv:hep-ph/0210213].
- [4] S. Frixione and B. R. Webber, *Matching NLO QCD computations and parton shower simulations*, JHEP **0206** (2002) 029 [arXiv:hep-ph/0204244]  
S. Frixione, P. Nason and B. R. Webber, *Matching NLO QCD and parton showers in heavy flavour production*, JHEP **0308** (2003) 007 [arXiv:hep-ph/0305252].
- [5] G. Davatz, A.S. Giolo Nicollerat, M. Zanetti, *Systematic uncertainty of the top background in the  $H \rightarrow WW \rightarrow$  Channel*, **CMS NOTE-2006-048**.
- [6] T. Sjöstrand *et al.*, Comput. Phys. Commun. 135 (2001) 238.
- [7] S.R. Slabospitsky, Comput. Phys. Commun. 148 (2002) 87.
- [8] F. Maltoni, in Proceedings of TOP2006 workshop.
- [9] J. Campbell and F. Tramontano, *Next-to-leading order corrections to  $Wt$  production and decay*, [arXiv:hep-ph/0506289].

- [10] J. Campbell and K. Ellis *Monte Carlo for FeMtobarn processes*, <http://mcfm.fnal.gov/>
- [11] **CMS NOTE-2006/019**, A. Rizzi, F. Palla and G. Segneri, *Track impact parameter based b-tagging with CMS*
- [12] F. Maltoni and T. Stelzer, JHEP **0302** (2003) 027 [arXiv:hep-ph/0208156].
- [13] N. Kauer *Top Background Extrapolation for  $H \rightarrow WW$  Searches at the LHC*, Phys. Rev. D **70** (2004) 014020 [arXiv:hep-ph/0404045].
- [14] J. Heyninck, in Proceedings of TOP2006 workshop.